Rat Hepatitis E Virus as Cause of Persistent Hepatitis after Liver Transplant

Siddharth Sridhar, Cyril C.Y. Yip, Shusheng Wu, Jianpiao Cai, Anna Jin-Xia Zhang, Kit-Hang Leung, Tom W.H. Chung, Jasper F.W. Chan, Wan-Mui Chan, Jade L.L. Teng, Rex K.H. Au-Yeung, Vincent C.C. Cheng, Honglin Chen, Susanna K.P. Lau, Patrick C.Y. Woo, Ning-Shao Xia, Chung-Mau Lo, Kwok-Yung Yuen

All hepatitis E virus (HEV) variants reported to infect humans belong to the species *Orthohepevirus A* (HEV-A). The zoonotic potential of the species *Orthohepevirus C* (HEV-C), which circulates in rats and is highly divergent from HEV-A, is unknown. We report a liver transplant recipient with hepatitis caused by HEV-C infection. We detected HEV-C RNA in multiple clinical samples and HEV-C antigen in the liver. The complete genome of the HEV-C isolate had 93.7% nt similarity to an HEV-C strain from Vietnam. The patient had preexisting HEV antibodies, which were not protective against HEV-C infection. Ribavirin was an effective treatment, resulting in resolution of hepatitis and clearance of HEV-C viremia. Testing for this zoonotic virus should be performed for immunocompromised and immunocompetent patients with unexplained hepatitis because routine hepatitis E diagnostic tests may miss HEV-C infection. HEV-C is also a potential threat to the blood product supply.

Hepatitis E virus (HEV) infects 20 million humans worldwide annually (*1*). HEV-infected persons usually have self-limiting acute hepatitis. However, persistent hepatitis can occur in HEV-infected immunocompromised patients who acquire infection by eating undercooked pork, rabbit, deer, camel, or boar meat (*2*–*6*). HEV transmission through blood product transfusion also has been described (*7*).

The diverse *Hepeviridae* family, which incorporates all HEV variants, includes members whose primary host species are terrestrial mammals (genus *Orthohepevirus*) and fish (genus *Piscihepevirus*) (*8*). The *Orthohepevirus* genus is classified into 4 species; HEV variants that have been reported to infect humans belong to *Orthohepevirus A* (HEV-A). Five genotypes within HEV-A (HEV-1–4 and -7) cause hepatitis in humans, and 3 genotypes (HEV-3, -4, and -7) can cause chronic hepatitis in immunocompromised patients after foodborne zoonotic transmission (*2*,*6*,*9*,*10*).

In addition to HEV-A, the *Orthohepevirus* genus includes 3 other species: *Orthohepevirus B* circulates in chickens, *Orthohepevirus C* (HEV-C) in rats and ferrets, and *Orthohepevirus D* in bats. HEV-C, also known as rat hepatitis E virus, shares only 50%–60% nt identity with HEV-A (*8*). The zoonotic potential of HEV-C is unknown; cases of clinical infection have not been reported. The substantial phylogenetic divergence between HEV-A and HEV-C, especially in critical receptor binding domains, forms a theoretical species barrier (*11*). Serologic and molecular tests for HEV are designed primarily to detect HEV-A, and they might miss HEV-C infections. Therefore, the threat to human health, including blood and organ supply safety, from HEV-C is unknown. We aimed to prove definitively that HEV-C can infect humans and describe the clinical, epidemiologic, genomic, and serologic features of this new zoonosis.

Materials and Methods

Study Population

We conducted this study in Queen Mary Hospital, a 1,700-bed tertiary care hospital in Hong Kong. We assessed 518 solid-organ transplant recipients (kidney, liver, lung, and heart transplant) who were followed up in Queen Mary Hospital for persistent biochemical hepatitis from January 1, 2014, or date of transplant (whichever date was later) through December 31, 2017. We defined persistent hepatitis as elevation of alanine aminotransferase (ALT) >1.5 times the upper limit of the reference level for a continuous period of ≥6 weeks. For patients whose ALT met this definition, we reviewed clinical records, ultrasonogram results, endoscopic retrograde cholangiopancreatography results, and laboratory results to identify the likely cause of hepatitis. We

Author affiliations: The University of Hong Kong, Hong Kong, China (S. Sridhar, C.C.Y. Yip, S. Wu, J. Cai, A.J.-X. Zhang, K.-H. Leung, T.W.H. Chung, J.F.W. Chan, W.-M. Chan, J.L.L. Teng, R.K.H. Au-Yeung, V.C.C. Cheng, H. Chen, S.K.P. Lau, P.C.Y. Woo, C.-M. Lo, K.-Y. Yuen); The University of Hong Kong–Shenzhen Hospital, Shenzhen, China (J.F.W. Chan, C.-M. Lo, K.-Y. Yuen); Xiamen University, Xiamen, China (N.-S. Xia)

DOI: https://doi.org/10.3201/eid2412.180937

considered patients to have hepatitis B virus (HBV), hepatitis C virus (HCV), or cytomegalovirus (CMV) reactivation if any of these viruses were detected in blood during the hepatitis episode. In patients with no identifiable cause of hepatitis, HEV IgM ELISA screening was performed, in accordance with the usual practice in Queen Mary Hospital. HEV infection was diagnosed if the HEV IgM assay was positive, and persistent HEV infection was diagnosed if HEV viremia in patient plasma lasted for ≥3 months. PCR sequencing was performed for speciation of HEV isolate. We obtained ethics approval from the Institutional Review Board of the University of Hong Kong/Hospital Authority West Cluster. We obtained written informed consent from all patients with persistent HEV infection.

Nucleic Acid Detection for Hepatitis Viruses and HEV Complete Genome Sequencing

We designed 3 in-house–developed reverse transcription PCRs (RT-PCRs) to detect HEV (online Technical Appendix Table 1, https://wwwnc.cdc.gov/EID/article/24/12/18-0937-Techapp1.pdf). Hepatitis A virus (HAV) RNA and CMV DNA detections were performed using in-house nucleic acid amplification tests. HBV and HCV viral loads were quantified using commercial kits (COBAS TaqMan, Roche, Basel, Switzerland; and RealTime HCV, Abbott, Chicago, IL, USA, respectively).

We sequenced the PCR product of the pan-*Orthohepevirus* RT-PCR using the RT-PCR primers. Because the RNA-dependent RNA polymerase sequences of patient HEV isolates clustered with rat HEV-C strains, primers for complete genome amplification were designed by multiple alignment of rat HEV-C genomes in GenBank (online Technical Appendix Table 2). We used these primers for complete genome sequencing of HEV in patient feces (strain LCK-3110). We constructed phylogenetic trees using MEGA6 with the general time reversible plus gamma model (*12*).

Cloning and Purification of Recombinant HEV-A and HEV-C Open Reading Frame 2 Protein

We used specific primers (online Technical Appendix) to amplify the genes encoding the 239 aa immunogenic recombinant peptides of HEV-A (genotype 4) and HEV-C. Cloning the amplified genes into a bacterial expression vector, expression in *Escherichia coli*, and protein purification were performed as previously described (*13*,*14*).

Antibodies Against HEV-A and HEV-C

Polyclonal antibodies against the HEV-C recombinant protein were raised in mice (online Technical Appendix). In addition, we used 2 murine monoclonal antibodies (mAbs) against open reading frame (ORF) 2 antigen of HEV-A in this study.

Serologic Testing

We conducted HEV antibody screening for patients with unexplained persistent hepatitis using HEV IgM and HEV IgG commercial ELISA kits (Wantai, Beijing, China) and detected hepatitis B surface antigen (HBsAg) using the ARCHITECT HBsAg chemiluminescent microparticle immunoassay (Abbott). HAV IgM and HCV antibodies were tested using VIDAS immunoassay kits (bioMérieux, Marcy-L'Étoile, France). For investigation of the HEV-C transmission event, we subjected patient and donor serum to HEV-A and HEV-C Western blots using polyclonal antiserum from mice inoculated with HEV-C protein and mAbs as controls. ELISAs using recombinant HEV-A and HEV-C protein-coated plates were designed based on the method described by Shimizu et al. with modifications (*15*). We set cutoffs and interpreted results to differentiate HEV-A– and HEV-C–specific serologic responses (online Technical Appendix).

Virus Culture

We selected cell lines A549 (lung adenocarcinoma), Huh-7 (hepatocellular carcinoma), and Caco-2 (colorectal adenocarcinoma) to investigate whether human cell lines could support HEV-C growth. Cell lines were chosen if they supported growth of patient-derived HEV isolates or HEV infectious clones (*16*–*18*) (online Technical Appendix). We subjected supernatants and lysates to HEV-C quantitative RT-PCR (qRT-PCR) and immunostaining.

Immunohistochemical and Immunofluorescence Staining

We conducted immunohistochemical staining of formalin-fixed paraffin-embedded liver tissue sections and infected A549 cell culture monolayers using HEV-C polyclonal serum antibodies and HEV-A mAbs. We performed immunofluorescence staining of permeabilized infected cells using HEV-C polyclonal antiserum (online Technical Appendix).

Epidemiologic and Environmental Investigation

We retrieved organ and blood donor serum for HEV ELISA, Western blot, and HEV-C qRT-PCR. To survey density of rat fecal contamination and collect environmental specimens for HEV-C qRT-PCR, we visited the patient's housing estate on November 22, 2017. Furthermore, from deep freezers we retrieved archived *Rattus* sp. liver, spleen, rectal swab, and kidney specimens collected during 2012–2017 within a 2.5-km radius around the patient's residence for preexisting pathogen surveillance programs and subjected them to HEV-C qRT-PCR. The HEV-C ORF2 fragment of qRT-PCR–positive specimens was sequenced using additional primers (online Technical Appendix Table 3).

Results

Hepatitis E Incidence in Transplant Recipient Cohort

Of 518 patients, 52 (10.2%) had persistent hepatitis (Table 1). Five (9.6%) patients with hepatitis tested positive for HEV IgM; 4 of these were kidney transplant recipients, and 1 was a liver transplant recipient. Together with reactivation of chronic HBV infection, HEV was the third most common cause of viral hepatitis in the local transplant population. Of the 5 patients, plasma HEV-A qRT-PCR of 3 renal transplant recipients was positive; another renal transplant recipient tested negative for HEV RNA. We have previously reported the clinical details of the 3 HEV-A–infected patients (*9*). Rat-derived HEV-C infection was diagnosed in the liver transplant recipient, which accounted for 1.9% (1/52) of persistent hepatitis in our cohort.

Patient History

A 56-year-old man underwent deceased-donor liver transplant on May 14, 2017, because of hepatocellular carcinoma complicating chronic HBV carriage. He received 1,000 mg hydrocortisone and 20 mg basiliximab (anti–interleukin-2 receptor mAb) as intraoperative antirejection prophylaxis and 4 units of platelets (derived from 4 separate blood donors) during the operation. His liver function tests (LFTs) reverted to normal, and he was discharged on posttransplant day 11. He was taking mycophenolate mofetil (500 mg 2×/d), tacrolimus (1 mg 2×/d), and prednisolone (5 mg 2×/d) as antirejection prophylaxis. He was also taking entecavir (0.5 mg 1×/d) for HBV suppression; serum HBsAg was negative 6 weeks after the transplant.

Routine phlebotomy on July 12 (day 59 posttransplant) revealed mild derangement of ALT to 74 U/L (reference 8–58 U/L). Other LFTs were normal. One week later, there was further derangement of parenchymal liver enzymes: ALT was 138 U/L, aspartate aminotransferase was elevated to 65 U/L (reference 15–38 U/L), γ-glutamyltransferase was 124 U/L (reference 11–62 U/L), and alkaline phosphatase was within reference limits at 70 U/L (reference 42–110 U/L). Complete blood count showed lymphopenia, at 0.88×10^9 cells/L, although total leukocyte count was within reference levels.

The patient was empirically managed for acute graft rejection with increased immunosuppression using a 3-day course of methylprednisolone. Valganciclovir was prescribed for low-level whole blood CMV viremia of 5.31×10^2 IU/mL. However, LFTs continued to deteriorate despite clearance of CMV viremia and increased immunosuppression. Liver biopsy showed nonspecific mild to moderate inflammatory infiltrate comprising small lymphocytes in the portal tracts. There were no viral inclusion bodies, and immunohistochemical staining for CMV and hepatitis B core antigens was negative. Results of testing for HBsAg in serum, HBV DNA in plasma, HCV antibody in serum, HAV IgM in serum, and HAV RNA in plasma and feces were all negative. HEV IgM was detected in serum collected on August 22 (day 100 posttransplant). Because of the serology result and ongoing LFT derangement, persistent HEV infection was suspected. A qRT-PCR targeting HEV-A was performed on patient fecal and plasma specimens; HEV-A RNA was not detected in either specimen. An RT-PCR capable of detecting all species within the *Orthohepevirus* genus detected amplicons (online Technical Appendix Figure 1) in plasma, feces, and liver tissue. Sequencing confirmed that the products clustered with rat HEV-C strains.

Table 1. Demographic and clinical characteristics of solid organ transplant recipients, Queen Mary Hospital, Hong Kong, January 1, 2014–December 31, 2017*

Characteristic	Result†
No. transplant recipients	518
Organ transplanted	
Kidney	430 (83.0)
Liver	61 (11.7)
Heart	16 (3.1)
Lung	10 (1.9)
Combined kidney and liver	1 (0.2)
Median age, y	56
Sex	
F	203 (39.2)
M	315 (60.8)
Prevalence of persistent biochemical hepatitis	52 (10.2)
Cause of biochemical hepatitis	
Viral hepatitis‡	
Reactivation of chronic HBV infection	5 (9.6)
Chronic HCV infection	7 (13.5)
Chronic HEV infection	5 (9.6)
CMV reactivation	8 (15.4)
Nonviral causes†	
Drug toxicity	7 (13.5)
Nonalcoholic fatty liver disease	3 (5.8)
Liver graft rejection	7 (13.5)
Biliary anastomotic stricture	5 (9.6)
Liver malignancies	2 (3.8)
Septic cholestasis	2 (3.8)
Recurrent pyogenic cholangitis	1 (1.9)

*CMV, cytomegalovirus; HBV, hepatitis B virus; HCV, hepatitis C virus; HEV, hepatitis E virus.
†All results are no. (%) unless otherwise indicated.
‡All percentages based on no. patients with biochemical hepatitis.

Viral RNA Kinetics and Effect of Ribavirin Therapy

The patient's archived serum, saliva, urine, feces, and nonfixed liver tissue samples were retrieved for HEV-C RNA load testing using HEV-C qRT-PCR (Figure 1, panel A). Two pretransplant serum samples and 1 serum sample collected on day 17 after transplant did not contain HEV-C RNA. The first specimen with detectable HEV-C RNA was a serum sample collected 43 days after transplant, which contained an RNA load of 9.48×10^2 copies/mL; this result preceded onset of LFT derangement by 3 weeks. After heightened immunosuppression in July

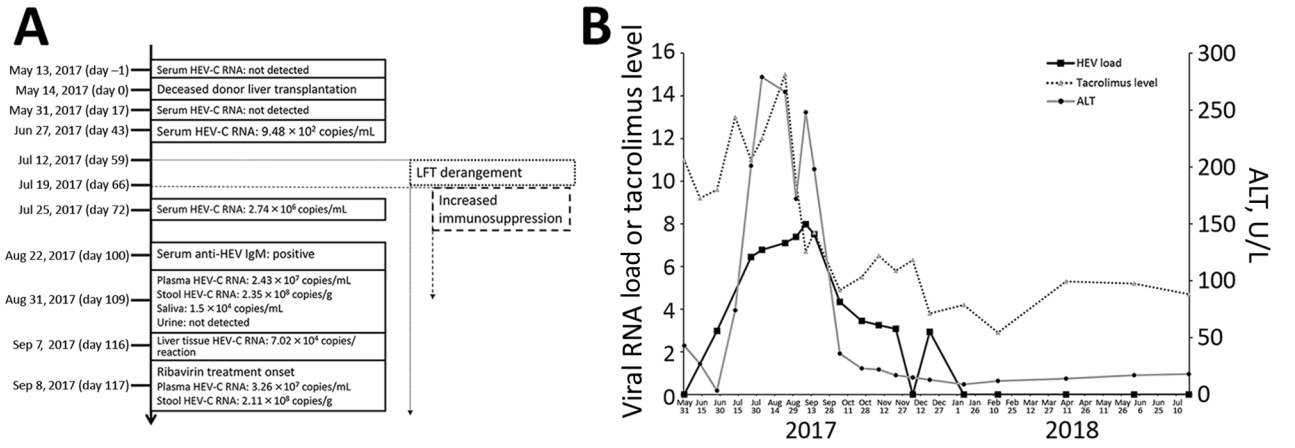

Figure 1. Natural course of HEV-C infection in a 56-year-old man at Queen Mary Hospital, Hong Kong. A) Timeline of major clinical events. All days are post transplant. B) Kinetics of liver function tests, tacrolimus levels (μg/L), and plasma HEV-C RNA load (log_{10} copies/mL) with relation to ribavirin therapy. ALT, alanine aminotransferase; HEV-C, *Orthohepevirus C*; LFT, liver function test.

and August, the HEV-C RNA load in blood steadily rose along with ALT (Figure 1, panel B). Variation in ALT correlated with the HEV-C RNA viral load by linear regression ($R^2 = 0.791$). HEV-C RNA was also detected in feces, saliva, and liver tissue (Figure 1, panel A); feces contained the highest RNA load.

Immunosuppressant dosages were decreased after confirmation of HEV infection. However, ALT and HEV-C RNA loads continued to increase despite reduction of plasma tacrolimus levels by 55% and rebound of lymphocyte count to 2.27×10^9 cells/L. Therefore, oral ribavirin 400 mg twice daily was started on September 7. ALT decreased within the first week after start of therapy and normalized within 1 month after starting ribavirin (Figure 1, panel B). HEV-C RNA loads also decreased to undetectable levels in plasma obtained on February 13, 2018. Ribavirin was stopped in April 2018, and HEV-C RNA in serum remained undetectable as of August 21, 2018, confirming sustained virologic response.

Serologic Analysis

We retrospectively tested all available patient serum and plasma samples for HEV IgG and IgM ELISA using the Wantai ELISA kit. The patient's serum before transplant was HEV IgG positive and IgM negative. HEV IgG and IgM optical density rose sharply from June 27, when HEV-C RNA was first detectable in blood, to July 25, when clinical hepatitis began (online Technical Appendix Figure 2). Despite high IgG levels, HEV-C RNA continued to rise until ribavirin was started.

To characterize the serologic response, Western blot using purified HEV-A and HEV-C recombinant proteins (Figure 2, panel A) was performed. Two mAbs raised against HEV-A were used: 1 produced a band in HEV-A IgG blot but not in the HEV-C blot (lane 8; Figure 2, panels B, C) confirming specificity, and the other was cross-reactive against HEV-A and HEV-C (lane 9; Figure 2, panels B, C). Polyclonal serum raised in mice inoculated with HEV-C protein reacted in both blots, showing that the serum was cross-reactive (lane 7). Patient serum collected on day 100 after transplant (lane 1) was tested against HEV-A and HEV-C recombinant proteins. The serum specimen showed reactivity in both Western blots.

Two patient serum samples, 1 obtained 3 months before transplant and the other obtained on day 100 after transplant, were tested in IgG ELISAs using HEV-A and HEV-C protein-coated plates. The pretransplant serum (Figure 2, panel D) had cross-reactive antibodies against both HEV-A and HEV-C proteins (<2-fold difference in titer using OD cutoff of 0.3). However, the posttransplant serum (Figure 2, panel E) showed >16-fold rise in HEV-A IgG titer and markedly higher reactivity against HEV-A than against HEV-C (>4-fold difference in titer using a cutoff OD of 0.3).

Liver Histologic and Immunohistochemical Analyses

Serial liver biopsies showed progressively worsening hepatocyte ballooning and degenerative changes (Figure 3, panels A, B). Apoptotic hepatocytes were identified in the biopsy obtained on day 98 posttransplant (Figure 3, panel B). Immunohistochemical staining with the cross-reactive mAb showed positive perinuclear cytoplasmic signals (Figure 3, panel C), and negative control with bovine serum albumin instead of mAb showed no signals (Figure 3, panel D).

Genomic Description

Complete genome sequencing of the patient's fecal HEV isolate (LCK-3110) showed that the genome was 6,942 bp

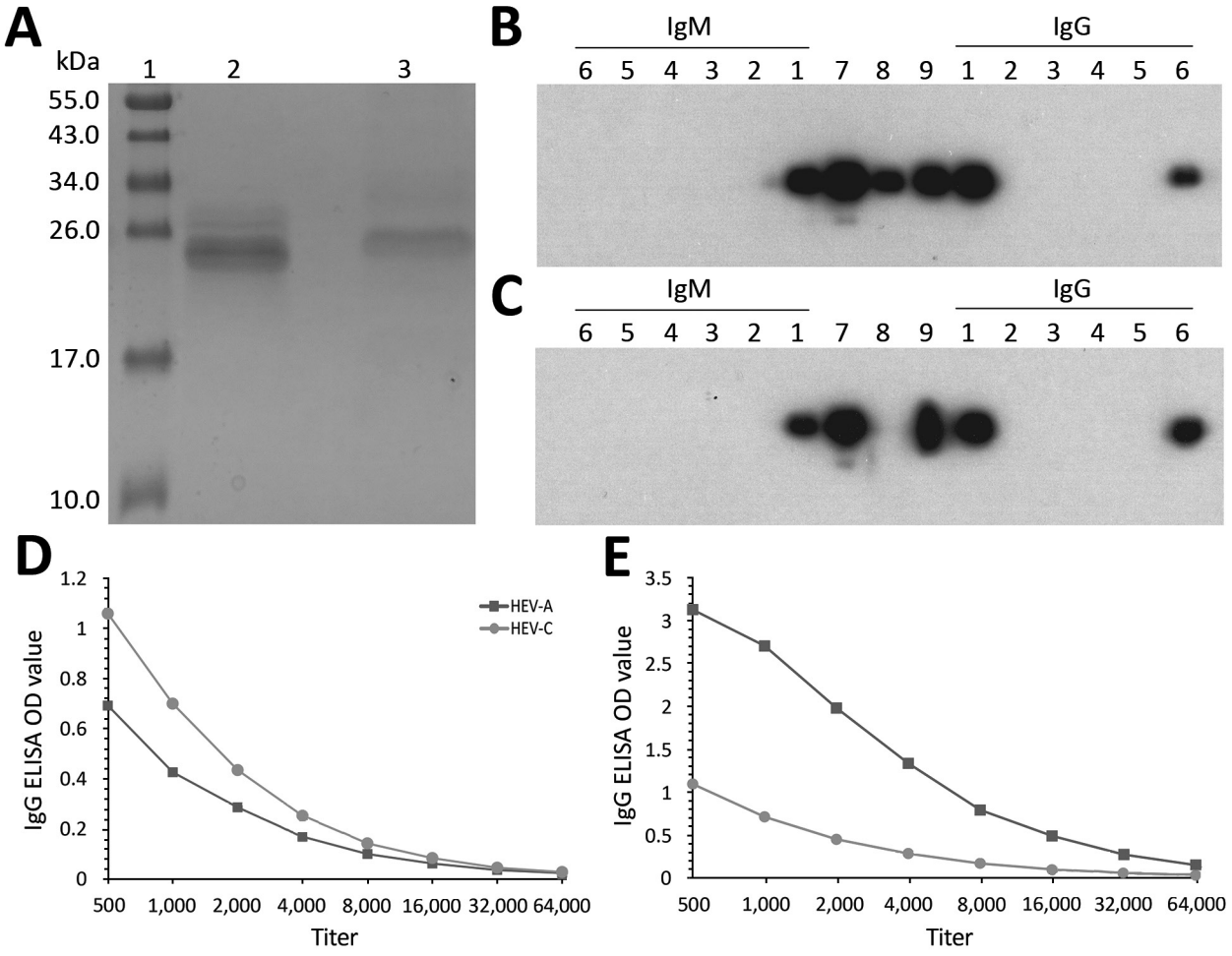

Figure 2. Serologic testing for HEV infection at Queen Mary Hospital, Hong Kong. A) Sodium dodecyl sulfate polyacrylamide gel electrophoresis gel showing purified HEV-A and HEV-C 239-aa recombinant proteins used in Western blot and ELISA. Lane 1, molecular weight marker; lane 2, HEV-A protein; lane 3, HEV-C protein. B–C) IgM and IgG Western blot using HEV-A protein (B) and HEV-C protein (C). Lane 1, patient serum (posttransplant day 100); lanes 2–5, individual platelet donor serum; lane 6, organ donor serum; lane 7, murine polyclonal serum against HEV-C; lane 8, specific monoclonal antibody against HEV-A; lane 9, cross-reactive monoclonal antibody against HEV-A and HEV-C. D, E) HEV-A and HEV-C ELISA IgG titers of patient pretransplant (D) and posttransplant serum (E) using an OD of 0.3 as assay cutoff as described in the online Technical Appendix (https://wwwnc.cdc.gov/EID/article/24/12/18-0937-Techapp1.pdf). HEV, hepatitis E virus; HEV-A, *Orthohepevirus A*; HEV-C, *Orthohepevirus C*; OD, optical density.

long (GenBank accession no. MG813927). Phylogenetic trees of the nucleotide and amino acid sequences of ORF1, ORF2, and ORF3 of HEV strains showed that LCK-3110 is most closely related to the Vietnam-105 strain (Figure 4; online Technical Appendix Figure 3, panels A, B), sharing 93.7% nt identity. Because no phylogenetic incongruence was found on comparison of trees of the 3 genomic segments, recombination was unlikely (Table 2; online Technical Appendix). To determine whether commonly used RT-PCRs for HEV nucleic acid amplification could detect HEV-C, we aligned published primer/probe sequences of HEV RT-PCRs (*19*–*22*) with complete genome sequences of HEV-A (genotype 1 reference strain) and HEV-C (strains LCK-3110, Vietnam-105, and LA-B350) using ClustalX 2.0 (http://www.clustal.org/clustal2/). Alignment revealed significant lack of homology with HEV-C at the 3′ end of either the forward or reverse primer for the assays described by Jothikumar et al. and Rolfe et al. (online Technical Appendix Figure 4, panels A, B) (*20*,*21*). Our in-house HEV-A qRT-PCR is based on the primer/probe design of Jothikumar et al. and was unable to detect HEV-C in patient specimens (*20*). For the assays described by Mansuy et al. and Colson et al. (*19*,*22*), there was significant lack of matching of probe sequence (40%–45% mismatch) to HEV-C genomes (online Technical Appendix Figure 4, panels C, D), which most likely would result in failure to detect any amplified nucleic acid.

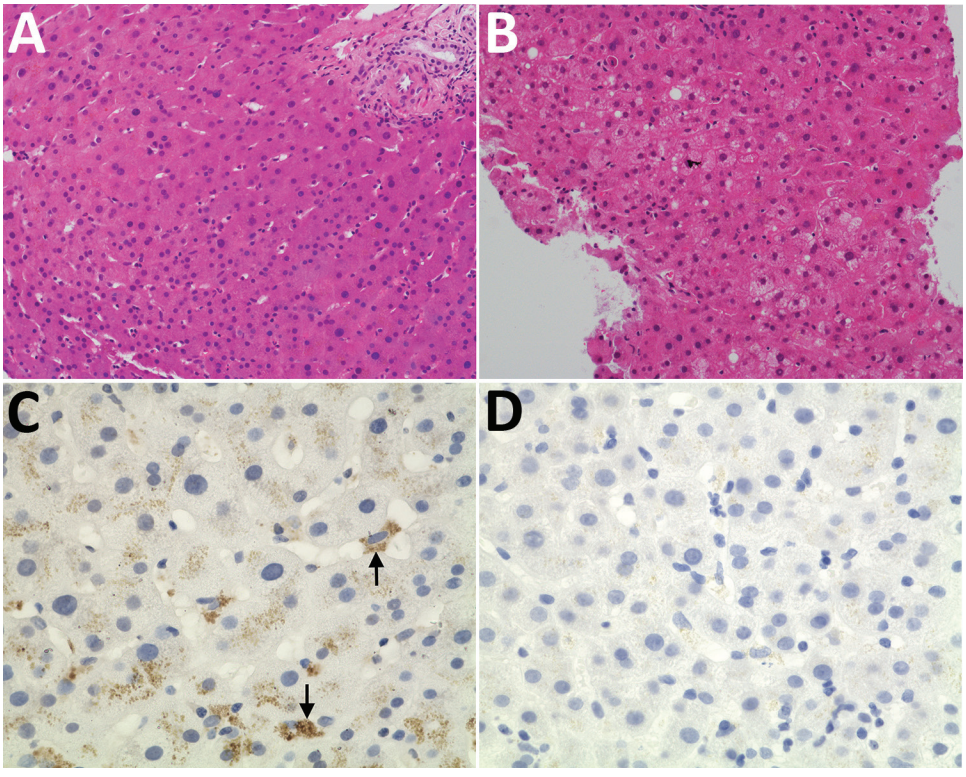

Figure 3. Histologic and immunohistochemical staining of liver tissue from a 56-year-old man at Queen Mary Hospital, Hong Kong. A, B) Liver tissue sections (original magnification ×200) stained with hematoxylin and eosin obtained at day 0 (A), showing normal hepatocyte architecture, and day 98 (B) after transplant showing progressive increase in hepatocyte ballooning and degenerative changes. C, D) Liver tissue section stained with cross-reactive monoclonal antibody (original magnification ×400); arrows show perinuclear antigen staining (C) and negative control with bovine serum albumin (D).

Virus Culture

We detected HEV-C RNA in supernatants from all 3 cell lines (Figure 5, panel A) inoculated with patient's feces at steady levels from day 3 to day 7 after inoculation. RNA loads in cell lysates were ≈1 log higher than concomitantly harvested supernatants, suggesting successful viral cell entry. Immunohistochemical staining (Figure 5, panels B, C) of A549 cell monolayers and immunofluorescence staining of infected Huh-7 and Caco-2 cells (online Technical Appendix Figure 5) confirmed the presence of cytoplasmic HEV ORF2 antigen when stained with antiserum against HEV-C. These findings suggested abortive viral replication of HEV-C in human cell lines.

Epidemiologic Investigation

The first clinical sample with detectable HEV-C RNA was obtained 43 days after transplant. HEV-C was not detected in serum samples obtained before transplant. Serum samples from the organ donor and all 4 platelet donors tested negative by IgM Western blot against HEV-C recombinant protein (Figure 2, panel C, lanes 2–6) and HEV-C qRT-PCR.

The patient's house unit was located adjacent to a refuse chute. He had noticed rodent droppings but had never seen rats inside his home. A site visit to the housing estate was conducted on November 22, 2017. Rodent droppings were found around refuse collection bins on the ground floor and the floor where the patient lived. Twelve rodent fecal specimens, 2 swab samples from the drain, and 2 swab samples from the refuse room floor tested negative for HEV-C RNA. To expand the investigation, we retrieved archived rodent samples collected from the area around the patient's housing estate (≈2.5-km radius) as part of preexisting pathogen surveillance programs. Spleen, kidney, liver, and rectal swab specimens from 27 rats were tested by qRT-PCR. The internal organs of 1 street rat (*Rattus norvegicus*) collected in 2012 tested positive for HEV-C RNA (strain name SRN-02). The ORF2 aa sequence of this isolate had 90.9% identity to LCK-3110.

Discussion

Discovered in Germany in 2010, rat HEV variants have been detected in rodent samples in Asia, Europe, and North America (*23*–*26*). Because of high divergence from human-pathogenic HEV, rat HEV has been classified into a separate species, *Orthohepevirus C*, within the family *Hepeviridae* (*27*). The zoonotic potential of HEV-C is controversial. Virus-like protein ELISAs show possible subclinical infection among forestry workers in Germany and febrile inpatients in Vietnam, although interpretation of such studies is difficult because of serologic cross-reactivity between HEV-A and HEV-C (*15*,*28*). Immunocompetent rhesus macaques do not appear to be susceptible to experimental infection with a North America HEV-C isolate (*23*).

In this study, we detected HEV-C RNA in multiple specimens from a transplant recipient. The HEV-C infection manifested as persistent hepatitis, as shown by temporal correlation between blood HEV-C RNA detection and

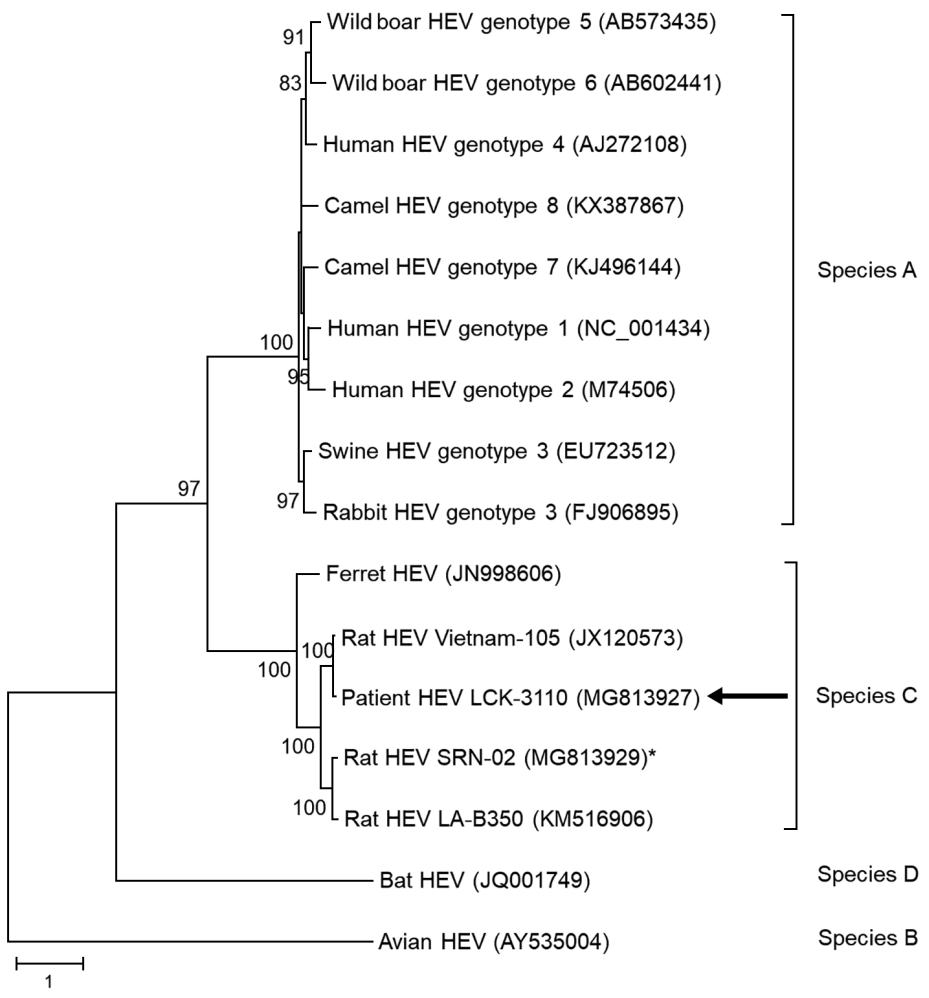

Figure 4. Phylogenetic analysis using complete open reading frame 2 nucleotide sequences of LCK-3110 and other hepatitis E virus strains. The tree was constructed using maximum-likelihood method with bootstrap values calculated from 1,000 trees. Only bootstrap values >70% are shown. GenBank accession numbers are provided. Arrow indicates strain LCK-3110; asterisk indicates strain SRN-02 detected in a street rodent in the epidemiologic investigation. Scale bar indicates mucleotide substitutions per site.

hepatitis onset, presence of HEV-C RNA in liver tissue, and normalization of liver function tests with viral clearance. These findings prove that HEV-C can infect humans to cause clinically significant illness and signal a need to reevaluate the importance of HEV-C as a human zoonosis among both immunocompromised and immunocompetent patients with hepatitis of unknown etiology.

The patient reported here acquired HEV-C infection despite having HEV IgG. Interpreted in parallel with the finding by Sanford et al. that inoculating pigs with HEV-C

Table 2. Comparison between nucleotide and deduced amino acid sequence identities of HEV strain LCK-3110 and other HEV strains

		Rat HEV strain LCK-3110						
		Entire	Nucleotides, %			Amino acids, %		
HEV strain (GenBank accession no.)	HEV species	genome	ORF1	ORF2	ORF3	ORF1	ORF2	ORF3
Genotype 1 (NC_001434)	HEV-A	57.6	56.4	60.9	55.0	50.0	56.3	31.0
Genotype 2 (M74506)	HEV-A	57.3	56.3	60.0	50.4	49.7	56.1	27.6
Genotype 3 (EU723512)	HEV-A	56.6	55.4	60.7	51.9	50.3	56.5	30.7
Genotype 4 (AJ272108)	HEV-A	56.5	55.4	59.8	55.4	49.7	56.4	31.0
Rabbit HEV (FJ906895)	HEV-A	56.0	54.9	59.9	51.6	50.1	56.4	27.6
Wild boar HEV (AB573435)	HEV-A	57.3	56.2	60.4	54.8	49.7	56.2	33.6
Wild boar HEV (AB602441)	HEV-A	56.8	55.7	59.6	54.5	50.3	56.5	31.9
Camel HEV (KJ496144)	HEV-A	55.9	54.9	59.4	53.5	50.5	56.2	32.2
Camel HEV (KX387867)	HEV-A	55.6	54.3	59.7	53.7	50.1	55.8	29.6
Rat HEV Vietnam-105 (JX120573)	HEV-C	93.7	93.3	95.2	96.4	98.2	98.0	95.1
Rat HEV LA-B350 (KM516906)	HEV-C	77.3	76.3	79.7	79.3	88.0	92.1	64.7
Ferret HEV (JN998606)	HEV-C	68.7	67.5	71.1	64.2	74.8	78.7	45.9
Bat HEV (JQ001749)	HEV-D	53.8	53.8	54.3	44.7	45.7	47.9	18.1
Avian HEV (AY535004)	HEV-B	53.5	54.0	53.0	46.4	45.6	43.5	24.8

*HEV, hepatitis E virus; ORF, open reading frame.

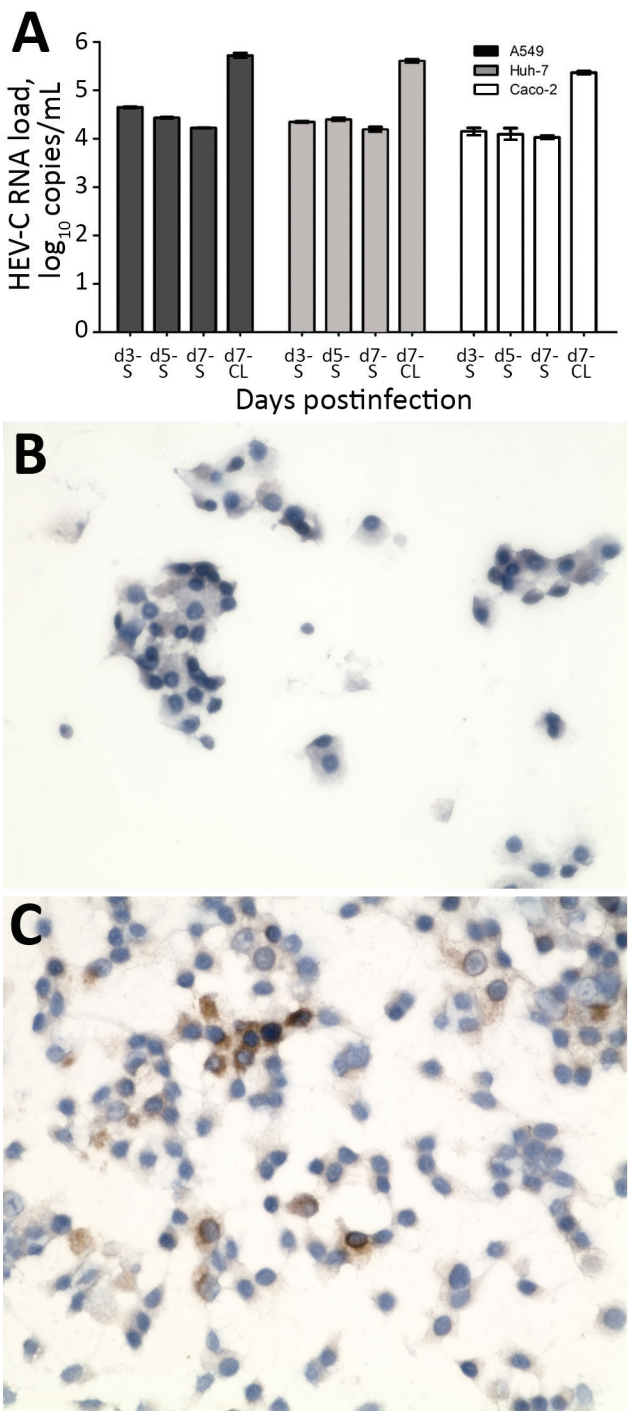

Figure 5. Isolation of HEV-C from 56-year-old male patient's feces in cell culture, Queen Mary Hospital, Hong Kong. A) HEV-C RNA loads in culture S and day-7 CL of A549, Huh-7, and Caco-2 cell lines after inoculation by patient's filtered fecal suspension. Mean of 3 replicates; error bars indicate SEM. B) Uninfected A549 cell monolayer stained with anti–HEV-C polyclonal antiserum. C) Infected A549 cell monolayer stained with anti–HEV-C polyclonal antiserum. Original magnification ×400. CL, cell lysate; HEV, hepatitis E virus; S, supernatant.

ORF2 protein did not protect them from HEV-A infection and low amino acid homology between HEV-A and HEV-C in critical immunogenic domains (*29*), our data suggest that HEV-A antibodies do not protect against HEV-C infection. The patient's postinfection serum showed significantly higher reactivity in an HEV-A–specific ELISA than in an HEV-C ELISA; the humoral immune responses of persons with past HEV-A infection to de novo HEV-C infection are worthy of further study to identify whether anamnestic responses are mounted.

The patient's HEV isolate had high nucleotide similarity to the HEV-C Vietnam-105 strain. It shared less homology with the North America LA-B350 strain, especially in the ORF3 domain, which is important for viral egress (*30*). Interspecies transmission could not be attributed to specific viral mutations. Future studies will need to include differences in zoonotic potential between HEV-C strains from Asia and the Americas.

The patient's immunosuppression possibly enabled the virus to surmount the species barrier, as described previously for avian influenza (*31*,*32*). HEV-C infections may go undiagnosed because of amplification failure in RT-PCRs, which are designed based on HEV-A sequences (online Technical Appendix Figure 3). The Wantai ELISA, based on HEV-A genotype 1, was able to detect IgM in this patient, but whether the assay is sensitive for HEV-C infection or was detecting only HEV-A–specific antibodies is uncertain. Therefore, we believe that specific RT-PCR is the most reliable method to diagnose HEV-C infections.

Our findings are also relevant to blood and organ donation safety. Because of the inability of commonly used RT-PCRs to detect HEV-C, transmission from asymptomatically infected immunocompetent donors may occur, even in countries that screen donated blood for HEV. Studies examining frequency of HEV-C contamination in blood products are needed to quantify this threat.

The patient lived in a housing estate with evidence of rat infestation in the refuse bins outside his home. We identified HEV-C in street rodents from the area, but the isolate was not closely related to the patient's isolate. The route of transmission is unclear; we postulate that contamination of food by infected rat droppings in the food supply is possible. Other possibilities include reactivation of a subclinical infection in the patient posttransplant or a donor-derived infection from residual HEV-C in the transplanted organ. However, we found no serologic or virologic evidence of HEV-C infection in donor and recipient serum before transplant. An occult infection in the donated liver, which reactivated after transplant as described previously for HEV-A, cannot be completely excluded. Detailed studies are needed to ascertain the route of HEV-C infection in humans.

Acknowledgment

We thank N.S. Xia for his kind gift of murine mAbs against HEV-A.

This study was supported by donations from Shaw Foundation and from Michael Seak-Kan Tong. The study was partially funded by the Consultancy Service for Enhancing Laboratory Surveillance of Emerging Infectious Disease for Department of Health of the Hong Kong Special Administrative Region of China, Seed Fund for Basic Research, and Enhanced New Staff Start-up Research Grant of the University of Hong Kong.

J.F.W.C. has received travel grants from Pfizer Corporation Hong Kong and Astellas Pharma Hong Kong Corporation Limited and was an invited speaker for Gilead Sciences Hong Kong Limited and Luminex Corporation.

About the Author

Dr. Sridhar is a clinical assistant professor at the Department of Microbiology, The University of Hong Kong. His major research interests include viral hepatitis and clinical virology.

References

1. Rein DB, Stevens GA, Theaker J, Wittenborn JS, Wiersma ST. The global burden of hepatitis E virus genotypes 1 and 2 in 2005. Hepatology. 2012;55:988–97. http://dx.doi.org/10.1002/hep.25505
2. Lee GH, Tan BH, Teo EC, Lim SG, Dan YY, Wee A, et al. Chronic infection with camelid hepatitis E virus in a liver transplant recipient who regularly consumes camel meat and milk. Gastroenterology. 2016;150:355–7.e3. http://dx.doi.org/10.1053/j.gastro.2015.10.048
3. Abravanel F, Lhomme S, El Costa H, Schvartz B, Peron JM, Kamar N, et al. Rabbit hepatitis E virus infections in humans, France. Emerg Infect Dis. 2017;23:1191–3. http://dx.doi.org/10.3201/eid2307.170318
4. Li TC, Chijiwa K, Sera N, Ishibashi T, Etoh Y, Shinohara Y, et al. Hepatitis E virus transmission from wild boar meat. Emerg Infect Dis. 2005;11:1958–60. http://dx.doi.org/10.3201/eid1112.051041
5. Tei S, Kitajima N, Takahashi K, Mishiro S. Zoonotic transmission of hepatitis E virus from deer to human beings. Lancet. 2003; 362:371–3. http://dx.doi.org/10.1016/S0140-6736(03)14025-1
6. Kamar N, Selves J, Mansuy JM, Ouezzani L, Péron JM, Guitard J, et al. Hepatitis E virus and chronic hepatitis in organ-transplant recipients. N Engl J Med. 2008;358:811–7. http://dx.doi.org/10.1056/NEJMoa0706992
7. Hewitt PE, Ijaz S, Brailsford SR, Brett R, Dicks S, Haywood B, et al. Hepatitis E virus in blood components: a prevalence and transmission study in southeast England. Lancet. 2014;384: 1766–73. http://dx.doi.org/10.1016/S0140-6736(14)61034-5
8. Sridhar S, Teng JLL, Chiu TH, Lau SKP, Woo PCY. Hepatitis E virus genotypes and evolution: emergence of camel hepatitis E variants. Int J Mol Sci. 2017;18:E869. http://dx.doi.org/10.3390/ijms18040869
9. Sridhar S, Chan JFW, Yap DYH, Teng JLL, Huang C, Yip CCY, et al. Genotype 4 hepatitis E virus is a cause of chronic hepatitis in renal transplant recipients in Hong Kong. J Viral Hepat. 2018;25:209–13. http://dx.doi.org/10.1111/jvh.12799
10. Sridhar S, Lo SK, Xing F, Yang J, Ye H, Chan JF, et al. Clinical characteristics and molecular epidemiology of hepatitis E in Shenzhen, China: a shift toward foodborne transmission of hepatitis E virus infection. Emerg Microbes Infect. 2017;6:e115. http://dx.doi.org/10.1038/emi.2017.107
11. Zhang J, Li SW, Wu T, Zhao Q, Ng MH, Xia NS. Hepatitis E virus: neutralizing sites, diagnosis, and protective immunity. Rev Med Virol. 2012;22:339–49. http://dx.doi.org/10.1002/rmv.1719
12. Tamura K, Stecher G, Peterson D, Filipski A, Kumar S. MEGA6: Molecular Evolutionary Genetics Analysis version 6.0. Mol Biol Evol. 2013;30:2725–9. http://dx.doi.org/10.1093/molbev/mst197
13. Chan JF, Yip CC, Tsang JO, Tee KM, Cai JP, Chik KK, et al. Differential cell line susceptibility to the emerging Zika virus: implications for disease pathogenesis, non-vector-borne human transmission and animal reservoirs. Emerg Microbes Infect. 2016;5:e93. http://dx.doi.org/10.1038/emi.2016.99
14. Chan JF, Chan KH, Choi GK, To KK, Tse H, Cai JP, et al. Differential cell line susceptibility to the emerging novel human betacoronavirus 2c EMC/2012: implications for disease pathogenesis and clinical manifestation. J Infect Dis. 2013; 207:1743–52. http://dx.doi.org/10.1093/infdis/jit123
15. Shimizu K, Hamaguchi S, Ngo CC, Li TC, Ando S, Yoshimatsu K, et al. Serological evidence of infection with rodent-borne hepatitis E virus HEV-C1 or antigenically related virus in humans. J Vet Med Sci. 2016;78:1677–81. http://dx.doi.org/10.1292/jvms.16-0200
16. Emerson SU, Nguyen HT, Torian U, Burke D, Engle R, Purcell RH. Release of genotype 1 hepatitis E virus from cultured hepatoma and polarized intestinal cells depends on open reading frame 3 protein and requires an intact PXXP motif. J Virol. 2010;84:9059–69. http://dx.doi.org/10.1128/JVI.00593-10
17. Emerson SU, Nguyen H, Graff J, Stephany DA, Brockington A, Purcell RH. In vitro replication of hepatitis E virus (HEV) genomes and of an HEV replicon expressing green fluorescent protein. J Virol. 2004;78:4838–46. http://dx.doi.org/10.1128/JVI.78.9.4838-4846.2004
18. Tanaka T, Takahashi M, Kusano E, Okamoto H. Development and evaluation of an efficient cell-culture system for Hepatitis E virus. J Gen Virol. 2007;88:903–11. http://dx.doi.org/10.1099/vir.0.82535-0
19. Mansuy JM, Peron JM, Abravanel F, Poirson H, Dubois M, Miedouge M, et al. Hepatitis E in the south west of France in individuals who have never visited an endemic area. J Med Virol. 2004;74:419–24. http://dx.doi.org/10.1002/jmv.20206
20. Jothikumar N, Cromeans TL, Robertson BH, Meng XJ, Hill VR. A broadly reactive one-step real-time RT-PCR assay for rapid and sensitive detection of hepatitis E virus. J Virol Methods. 2006;131:65–71. http://dx.doi.org/10.1016/j.jviromet.2005.07.004
21. Rolfe KJ, Curran MD, Mangrolia N, Gelson W, Alexander GJ, L'estrange M, et al. First case of genotype 4 human hepatitis E virus infection acquired in India. J Clin Virol. 2010;48:58–61. http://dx.doi.org/10.1016/j.jcv.2010.02.004
22. Colson P, Coze C, Gallian P, Henry M, De Micco P, Tamalet C. Transfusion-associated hepatitis E, France. Emerg Infect Dis. 2007;13:648–9. http://dx.doi.org/10.3201/eid1304.061387
23. Purcell RH, Engle RE, Rood MP, Kabrane-Lazizi Y, Nguyen HT, Govindarajan S, et al. Hepatitis E virus in rats, Los Angeles, California, USA. Emerg Infect Dis. 2011;17:2216–22. http://dx.doi.org/10.3201/eid1712.110482
24. Wang B, Cai CL, Li B, Zhang W, Zhu Y, Chen WH, et al. Detection and characterization of three zoonotic viruses in wild rodents and shrews from Shenzhen city, China. Virol Sin. 2017;32:290–7. http://dx.doi.org/10.1007/s12250-017-3973-z
25. Mulyanto, Depamede SN, Sriasih M, Takahashi M, Nagashima S, Jirintai S, et al. Frequent detection and characterization of hepatitis E virus variants in wild rats (*Rattus rattus*) in Indonesia. Arch Virol. 2013;158:87–96.
26. Johne R, Plenge-Bönig A, Hess M, Ulrich RG, Reetz J, Schielke A. Detection of a novel hepatitis E-like virus in faeces of wild rats

using a nested broad-spectrum RT-PCR. J Gen Virol. 2010;91:750–8. http://dx.doi.org/10.1099/vir.0.016584-0
27. Smith DB, Simmonds P, Jameel S, Emerson SU, Harrison TJ, Meng XJ, et al.; International Committee on Taxonomy of Viruses Hepeviridae Study Group. Consensus proposals for classification of the family *Hepeviridae.* J Gen Virol. 2014;95:2223–32. http://dx.doi.org/10.1099/vir.0.068429-0
28. Dremsek P, Wenzel JJ, Johne R, Ziller M, Hofmann J, Groschup MH, et al. Seroprevalence study in forestry workers from eastern Germany using novel genotype 3- and rat hepatitis E virus-specific immunoglobulin G ELISAs. Med Microbiol Immunol (Berl). 2012;201:189–200. http://dx.doi.org/10.1007/s00430-011-0221-2
29. Sanford BJ, Opriessnig T, Kenney SP, Dryman BA, Córdoba L, Meng XJ. Assessment of the cross-protective capability of recombinant capsid proteins derived from pig, rat, and avian hepatitis E viruses (HEV) against challenge with a genotype 3 HEV in pigs. Vaccine. 2012;30:6249–55.
30. Ding Q, Heller B, Capuccino JM, Song B, Nimgaonkar I, Hrebikova G, et al. Hepatitis E virus ORF3 is a functional ion channel required for release of infectious particles. Proc Natl Acad Sci U S A. 2017;114:1147–52. http://dx.doi.org/10.1073/pnas.1614955114
31. Cheng VC, Chan JF, Wen X, Wu WL, Que TL, Chen H, et al. Infection of immunocompromised patients by avian H9N2 influenza A virus. [Erratum in: Proc Natl Acad Sci U S A. 2017]. J Infect. 2011;62:394–9. http://dx.doi.org/10.1016/j.jinf.2011.02.007
32. Chen Y, Liang W, Yang S, Wu N, Gao H, Sheng J, et al. Human infections with the emerging avian influenza A H7N9 virus from wet market poultry: clinical analysis and characterisation of viral genome. Lancet. 2013;381:1916–25. http://dx.doi.org/10.1016/S0140-6736(13)60903-4

Address for correspondence: Kwok-Yung Yuen, The University of Hong Kong, Carol Yu Centre for Infection, State Key Laboratory of Emerging Infectious Diseases, Department of Microbiology, Li Ka Shing Faculty of Medicine, Queen Mary Hospital, 120 Pokfulam Rd, Pokfulam, Hong Kong HK1, China; email: kyyuen@hkucc.hku.hk

Article DOI: https://doi.org/10.3201/eid2412.180937

Rat Hepatitis E Virus as Cause of Persistent Hepatitis after Liver Transplantation

Technical Appendix

Detailed Study Methods

HEV Real-Time Reverse Transcription PCR (qRT-PCR)

200 μL of each sample was subjected to total nucleic acid extraction into 60 μL eluate using the EZ1 Virus Mini Kit v2.0 (Qiagen, Hilden, Germany). Primer & probe sequences, gene targets and product size of the 2 qRT-PCR assays specific for HEV-A and HEV-C are included in Technical Appendix Table 1. Quantitative real-time RT-PCR (qRT-PCR) assays were performed using QuantiNova Probe RT-PCR Kit (Qiagen) in a LightCycler 480 Real-Time PCR System (Roche, Basel, Switzerland). Each 20 μL-reaction mix contained 1× QuantiNova Probe RT-PCR Master Mix, 1× QN Probe RT-Mix, 0·8 μM forward and reverse primers, 0·2 μM probe and 5 μl template RNA. Reactions were incubated at 45°C for 10 min and 95°C for 5 min, followed by 50 cycles at 95°C for 5 s and 55°C for 30 s. Quantitation was achieved using plasmid standards prepared using the pCRII-TOPO vector (Invitrogen, Carlsbad, CA, USA) cloned with the target insert. Plasmid concentrations ranging from 10^2–10^6 copies/reaction were used to generate standard curves for each qRT-PCR run.

HEV Conventional RT-PCR

Conventional RT-PCR for HEV RNA detection in plasma, stool and liver biopsy samples was performed using primers listed in Technical Appendix Table 1. Reverse transcription for the pan-*Orthohepevirus* conventional RT-PCR assay was performed using the SuperScript III kit (Invitrogen). The reaction mixture (10 μL) contained RNA, first-strand buffer (50 mM Tris-HCl pH 8.3, 75 mM KCl, 3 mM MgCl2), 5 mM DTT, 50 ng random hexamers, 500 μM of each deoxynucleoside triphosphate (dNTP) and 100 U Superscript III reverse transcription. The mixtures were incubated at 25°C for 5 min, followed by 50°C for 60 min and 70°C for 15 min.

The PCR mixture (25 μL) contained cDNA, 1× PCR buffer II (10 mM Tris-HCl [pH 8.3], 50 mM KCl), 2 mM MgCl2, 200 μM of each dNTP, 1 μM forward and reverse primers and 1.0 U of Taq polymerase (Applied Biosystems, Foster City, CA, USA). PCR was performed using an automated thermocycler (Applied Biosystems) with a hot start at 95°C for 10 min, followed by 40 cycles of 94°C for 1 min, 55°C for 1 min, and 72°C for 1 min and a final extension at 72°C for 10 min. The PCR products were detected by agarose gel electrophoresis (staining gel with ethidium bromide, followed by visualization under UV light).

HEV Complete Genome Sequencing

PCR amplicon of the pan-*Orthohepevirus* RT-PCR assay was extracted using the QIAquick gel extraction kit (Qiagen). Both strands of the PCR product were sequenced twice with an ABI Prism 3130xl DNA Analyzer (Applied Biosystems) using primers listed in Technical Appendix Table 1. As the 235 bp RNA-dependent RNA polymerase (RdRp) sequences of HEV isolates obtained from patient specimens clustered with rat HEV-C strains, degenerate primers for complete genome amplification were designed by multiple alignment of the rat HEV-C genomes available in GenBank as per Technical Appendix Table 2. RNA extracted from the patient's stool (containing HEV isolate LCK-3110) was converted to cDNA by a combined random-priming and oligo(dT) priming strategy; this cDNA was used as the template for complete genome sequencing. The 5′ end of LCK-3110 was confirmed by rapid amplification of cDNA ends using Terminal Deoxynucleotidyl Transferase, recombinant (Invitrogen). Sequences were assembled and manually edited to produce final sequences of the viral genomes by BioEdit version 7.2.5 (NC State University, Raleigh, NC, USA).

HEV-A and HEV-C Peptide Expression

(5′-CATATGCTGTTAGGCGGCCTGCCAAC-3′ and 5′-CTCGAGCATCGGCACTGCAGCCGAG-3′) were used to amplify the gene encoding the 239-aa (aa) recombinant peptide corresponding to aa 368–606 of HEV-C ORF2. Primers (5′-CATATGATAGCATTGACCCTGTTTAATCT-3′ and 5′-CTCGAGAGCAGAGTGGGGTGCTAAAACAC-3′) were used to amplify the HEV-A gene encoding the recombinant peptide corresponding to aa 413–651 of HEV-A ORF2 (genotype 4). Amplified genes were cloned into the *Nde I* and *Xol I* sites of bacterial expression vector pETH in frame and downstream of the series of 6 histidine residues. The recombinant 239 aa HEV-A

and HEV-C proteins were expressed in *Escherichia coli* and purified by using the Ni-nitrilotriacetic acid affinity chromatography assay (Qiagen) according to manufacturer instructions. The HEV-A and HEV-C proteins had a 219 aa overlapping fragment and shared 52% sequence homology. The sequence alignment of the 2 proteins is as follows:

```
HEV-A      IALTLFNLADTLLGGLPTELISSAGGQLFYSRPVVSANGEPTVKLYTSVENAQQDKGIAI 60
HEV-C     ----LLGGLPTDLVSNAGGQLFYGRPQVSENGEPSVKLYTSVEAAQLDHGVTI         49
                  *******:*:*.*******.** ** ****:******** ** *:*::*

HEV-A      PHDIDLGESRVVIQDYDNQHEQDRPTPSPAPSRPFSVLRANDVLWLSLTAAEYDQTTYGS 120
HEV-C      PHDIDLGVSAITLQDFDNQHLQDRPTPSPAPARPITNWRSGDVVWVTLPSAEYAQSQSAM 109
           ******* *:.:**:**** **********:**::  *:.**:*::*:*** *:  .

HEV-A      STNPMYVSDTVTFVNVATGAQGVARSLDWSKVTLDGRPLTTIQQYSKTFFVLPLRGKLSF 180
HEV-C      GSHPAYWSEEATIINVATGQRAAVSSIKWDQVTLNGKALHKETHSGLVYYQLPLMGKINF 169
           .::* * *: .*::*****:... *:.*.:***:*: * . : . .:: *** **:.*

HEV-A      WEAGTTKAGYPYNYDTTASDQILIENAAG-HRVCISTYTTNLGSGPVSISAVGVLAPHS  238
HEV-C      WQQGTTKAGYTYNYNTTDSDSLWVWWDGGSKAYLYISTYTTMLGAGPVNITGLGAVGPNP 229
           *: ******* ***:** **.::   .*   : ****** **:***.*:.:*.:.*:

HEV-A      A----                                                        239
HEV-C      VDQASAAVPM                                                   239
```

Antibodies Against HEV-A and HEV-C

Thirty micrograms of purified recombinant HEV-C protein mixed with an equal volume of complete Freund's adjuvant (Sigma-Aldrich, St. Louis, MO, USA) was injected subcutaneously into mice followed by 4 injections of incomplete Freund's adjuvant (Sigma-Aldrich) at 14-day intervals. Polyclonal antiserum collected after the fourth injection were used for serologic and immunohistochemical assays.

HEV In-House Serologic Assays

For the Western blot assay, purified recombinant HEV-A and HEV-C proteins were separated electrophoretically in a 12% gel and transferred to a nitrocellulose membrane. Western blot was performed in a Mini-PROTEAN II Multiscreen Apparatus (Bio-Rad, Hercules, CA, USA). The membrane was incubated with polyclonal anti-serum (dilution of 1:10,000) from mice immunized with purified HEV-A and HEV-C proteins, monoclonal antibodies (1 μg/mL) against HEV-A, patient and organ/blood donor serum (in dilution of 1:500) for 1 h at 37°C. After washing, the membrane was incubated with horseradish peroxidase (HRP; Sigma-Aldrich) conjugated goat anti-human (IgG or IgM) and goat anti-mouse antibodies for 30 min at 37°C, and developed by incubation with Advansta ECL WesternBright Quantum Detection Kit (Advansta, Menlo Park, CA, USA).

For the HEV-A and HEV-C in-house ELISAs, 96-well microwell plates (Costar, Corning, NY, USA) were coated with purified recombinant HEV-A and HEV-C proteins. 100 μL of serum from three asymptomatic blood donors who tested negative in the Wantai HEV IgG ELISA and both HEV-A and HEV-C IgG Western blots was diluted 1:500 in 0.1% bovine serum albumin (BSA). Diluted serum was added to the ELISA plates (2 replicates) and incubated at 37°C for 1 h. After a washing step, goat anti-human-horse radish peroxidase (100 μL/ well) was added to plates followed by incubation at 37°C for 30 min. After washing, tetramethylbenzidate substrate was added. The reaction was stopped after 10 min by addition of 0.3 N sulphuric acid. Plates were examined in an ELISA plate reader at 450 nm. The mean optical density (OD) of these negative control sera was 0.152 (range 0·132–0·171; SD ± 0.017) for HEV-C ELISA and 0.178 (range 0.169–0.187; SD ± 0·008). Based on these findings, a tentative ELISA cutoff of 0.3 was designated. As subsequent ELISA experiments were quantal measurements using serial dilutions of patient serum, a precise cutoff is not necessary. For the ELISA experiment, patient serum was serially diluted 2-fold from 1:500 to 1:64,000 in BSA followed by HEV-A and HEV-C IgG ELISA as described above. The OD values were plotted against serum dilution. The IgG titer of a serum specimen was defined as the reciprocal of the highest dilution that gave an OD value above the cutoff. Using the tentative cutoff of 0.3, a serum sample would be considered to be specifically reactive against a particular HEV antigen (i.e., HEV-A or HEV-C) if there was a 4-fold difference in IgG titers between the 2 ELISAs. For example, if the IgG titer above the

cutoff line was 4,000 by HEV-A ELISA and 8,000 by HEV-C ELISA, the serum would not be considered to be more reactive against 1 HEV antigen over the other. Conversely, if the HEV-A ELISA IgG titer was 4,000 and HEV-C ELISA IgG titer was 16,000, then the serum would be considered to be more reactive against HEV-C than HEV-A.

Cell Culture

The patient's stool was diluted in phosphate buffered saline (PBS) and filtered to produce a 10% suspension. The suspension was further diluted 1:10 (for A549 and Huh-7) and 1:100 (for Caco-2) and 300 μL of suspension was used to inoculate cells in 12-well plates at an estimated multiplicity-of-infection of 5 HEV genome equivalents/ cell. Inoculum was removed after 1 h and replaced with minimum essential medium supplemented with 1% fetal calf serum. Cell lines were incubated at 37°C and were examined for cytopathic effect (CPE) daily. On day 3 and day 5, 250 μL of supernatant was collected and replenished with fresh medium. Cell monolayers were maintained for 7 d before harvesting of cell lysate. A549 cell monolayers were inoculated in chamber wells for immunohistochemical staining.

Immunohistochemical and Immunofluorescence Staining

Immunofluorescence staining of infected and uninfected A549, Huh-7, and Caco-2 7-day cell lysates was performed using anti-HEV-C polyclonal serum and anti-HEV-A monoclonal antibody. Briefly, infected and uninfected cells (as a negative control) were washed twice with PBS and fixed on slides in cold acetone at –20°C for 10 min. Monolayers were then inoculated with mouse serum (diluted 1:100) for 1 h at 37°C. After washing 3 times with PBS, cells were incubated with FITC-conjugated goat anti-mouse IgG antibody (Invitrogen) (1:40 dilution) for 30 min. After washing 3 times in PBS, the cells were counter-stained with 0.25% Evans Blue for 15 min. After a final washing step and addition of mounting fluid, stained cells were visualized using a fluorescence microscope. Cells showing apple-green fluorescence in the cytoplasm were considered to be HEV infected.

De-paraffinized liver tissue sections were treated with antigen unmasking buffer (Vector Laboratories, Burlingame, CA, USA) and hydrogen peroxide block. Slides were then incubated with primary reagent (either cross-reactive monoclonal antibody or bovine serum albumin) overnight at 4°C. After rinsing, slides were incubated with biotin conjugated goat anti-mouse IgG at room temperature for 30 min. Rinsed slides were then incubated with HRP-streptavidin

followed by color development using 3, 3′-diaminobenzidine (Vector Laboratories). Liver tissue section slides were counterstained with Gill's hematoxylin and examined using light microscopy.

Description of LCK-3110 Complete Genome

Predicted genomic organization of LCK-3110 was similar to other rat HEV isolates: from 5′ to 3′ ends, it consists of a 5′-untranslated region at nucleotide positions 1–10, ORF1 at nt 11–4903, ORF3 at nt 4920–5228 overlapping with ORF2 at nt 4931–6865 and 3′ UTR at nt 6866–6942 (including poly-A tail). An additional putative ORF, corresponding to ORF4 (nt 27–578) in the Vietnam-105 rat HEV-C strain genome (GenBank accession no. JX120573), was also found in LCK-3110. LCK-3110 is most closely related to the Vietnam-105 strain, sharing a nucleotide identity of 93.7%. No phylogenetic incongruence was found on comparison of trees of the 3 genomic segments, therefore recombination was unlikely.

Alignment of the 151-aa segment corresponding to the highly immunogenic E2s domain of HEV-A ORF2 (aa 455–aa 603 of HEV-A genotype 1 sequence) showed 98.6% homology between the LCK-3110 and Vietnam-105 strains. On the other hand, homology between LCK-3110 and HEV-A genotype 1 (Xinjiang strain; GenBank accession no. NC001434) E2s domain was only 47.7%, which was even lower than the overall ORF2 sequence amino acid homology. In-silico epitope analysis of the target residue sites of the 8C11 HEV-A neutralizing monoclonal antibody showed that only 1 out of 6 residues were conserved between LCK-3110 and the Xinjiang strain with a serine to glutamic acid substitution at the critical host-specificity defining residue aa 497 (HEV-A genotype 1 numbering).

Technical Appendix Table 1. Primers and probes targeting hepatitis E*

HEV species targeted (gene target)		Primer/probe sequence (5′→3′)	Product size, bp	PCR methodology
Pan-*Orthohepevirus* (RdRp)	Forward	ATGGTAAAGTGGGNCARGGNAT	235	Conventional
	Reverse	CCAAGCGAGAAATTRTTYTGNGT		PCR
Orthohepevirus A (ORF2)	Forward	GGTGGTTTCTGGGGTGAC	70	qRT-PCR
	Reverse	AGGGGTTGGTTGGATGAA		
	Probe	FAM- TGATTCTCAGCCCTTCGC -BHQ1		
Orthohepevirus C (ORF1)	Forward	CTTGTTGAGCTYTTCTCCCCT	69	qRT-PCR
	Reverse	CTGTACCGGATGCGACCAA		
	Probe	HEX- TGCAGCTTGTCTTTGARCCC -IABkFQ		

*ORF, open reading frame; qRT-PCR; quantitative real-time reverse transcription PCR; RdRp: RNA-dependent RNA polymerase.

Technical Appendix Table 2. Primers used for complete genome sequencing of LCK-3110*

Primer name	Sequence (5′ - 3′)	Position
LPW418	GACCACGCGTATCGATGTCGACTTTTTTTTTTTTTTTV	1st round PCR for 5′ and 3′ ends
ratHEV-5RACE-R1	GTGAATGACATTGGCGTGCT	303–322 (1st round)
LPW417	GACCACGCGTATCGATGTCGAC	nested PCR for 5′ and 3′ ends
ratHEV-5RACE-R2	CGGATGCGACCAAGAAACAG	189–208 (nested)

Primer name	Sequence (5′ - 3′)	Position
ratHEV-1F	CGATGGAGACCCATCAGTATGT	9–30
ratHEV-1R	GCGTATARAGTGTGCATNCCATG	551–573
ratHEV-16F	ACATCCGCCGTTGCATTCT	396–414
ratHEV-16R	ACTCTGGTCGCCTTAATCCA	725–744
ratHEV-2F	GATCTACATCCGCGTGAGGT	512–531
ratHEV-2R	TAAAAMCCTGCYGAAACCCA	1340–1359
ratHEV-3F	CACGCAGGGYATATCWATGGG	1183–1203
ratHEV-3Rm	ATGAAACAACCGCACACCTG	1466–1485
ratHEV-10F	TGGGTTTCRGCAGGKTTTTA	1340–1359
ratHEV-10R	ATYGGGCCMGGTGTCCAAGA	1856–1875
ratHEV-18F	CGGTATGAAGTTGGCAGGCT	1642–1661
ratHEV-18R	CGTGTATTATCGGCCTGGGT	2260–2279
ratHEV-4F	GATGGBGCAGCNGTTTATGA	2075–2094
ratHEV-4Rm	AACCARGCYTGCATGGACTC	2411–2430
ratHEV-24F	GATTATAGGGTCCGCCAAGA	2291–2310
ratHEV-26R	GGTACAATAACCAGGTCACAGTC	2798–2820
ratHEV-5F	AAGTTTRTTGGYAATGCCCA	2699–2718
ratHEV-19R	GTGGTAGACATCCCTGGGTA	3131–3150
ratHEV-11F	CTAGARCCCACRGARTGGCG	3059–3078
ratHEV-11R	GTKATCGANCCAGGGTGCAT	3230–3249
ratHEV-20F	GATGTTCACCGGGGACAGT	3172–3190
ratHEV-20R	TTGGCGACTATGGCCTTCTC	4097–4116
LPW7308 (F)	ATGGTAAAGTGGGNCARGGNAT	4020–4041
LPW7311 (R)	CCAAGCGAGAAATTRTTYTGNGT	4232–4254
ratHEV-12F	GCGTGCAGAGTGTTTGAAAATGA	4190–4212
ratHEV-12R	GAACAGCAAAAGCACGAGCA	4947–4966
ratHEV-13Fm	GCGGATGGAACTCAAGGAAT	4843–4862
ratHEV-13R	ATTGGCGACTGCCCGGCATC	5207–5226
ratHEV-21F	GCTATCACCAACCAACCCTT	5095–5114
ratHEV-21R	GGTGGACGTGATGGAGTTC	5569–5587
ratHEV-14F	CGACTGAGGCYTCNAATTATGC	5424–5445
ratHEV-14R	TGCACRTCCTGCATRAACC	5940–5958
ratHEV-22F	ACACCCGGTAATACCAACAC	5831–5850
ratHEV-22R	ATAGTCGCCTCCTCGGACCA	6377–6396
ratHEV-15F	TCCGGYGATGTKGTGTGGGT	6296–6315
ratHEV-15R	ACTCGCGCMATAGCWTCAGC	6809–6828
ratHEV-23F1	TTTGTGGGTGTGGTGGGATG	6601–6620 (1st round)
ratHEV-23F2	GGGCTCTAAGGCTTATCTCTAT	6622–6643 (nested)

*Primer position corresponding to the genome sequence of HEV strain LCK-3110. Primers were derived from the following HEV-C sequences in GenBank: Vietnam-105 (GenBank accession no. JX120573), ratELOMB-131 (GenBank accession no. LC145325), ratIDE079F (GenBank accession no. AB847305), rat/R63/DEU/2009 (GenBank accession no. GU345042), LA-B350 (GenBank accession no. KM516906), and rat/Mu09/0685/DEU/2010 (GenBank accession no. JN167537). F, forward; HEV, hepatitis E virus; R, reverse.

Technical Appendix Table 3. Primers used for sequencing of open reading frame 2 of street rodent isolate SRN-02*

Rat HEV	Primer	Sequence 5′→3′
SRN-02	HEV-8F	GACTCTGACHGTCCCTCAGTC
	HEV-8R	GTAATGTVACCCACACMACATC
	HEV-9F	GCTGTSAGGTTYATGCAGGA
	LPW418	GACCACGCGTATCGATGTCGACTTTTTTTTTTTTTTTV
	LPW417	GACCACGCGTATCGATGTCGAC
	HEV-7F	TGGAACACNGTCTGGAAYATGGC
	HEV-12R	GAACAGCAAAAGCACGAGCA
	LPW36773	GCCGTATGGAGCTGAAGGA
	LPW36725	CGCATACCCACCCACCGAGT
	LPW36726	TGTGGGTCTGGTGGGATGG

*HEV, hepatitis E virus.

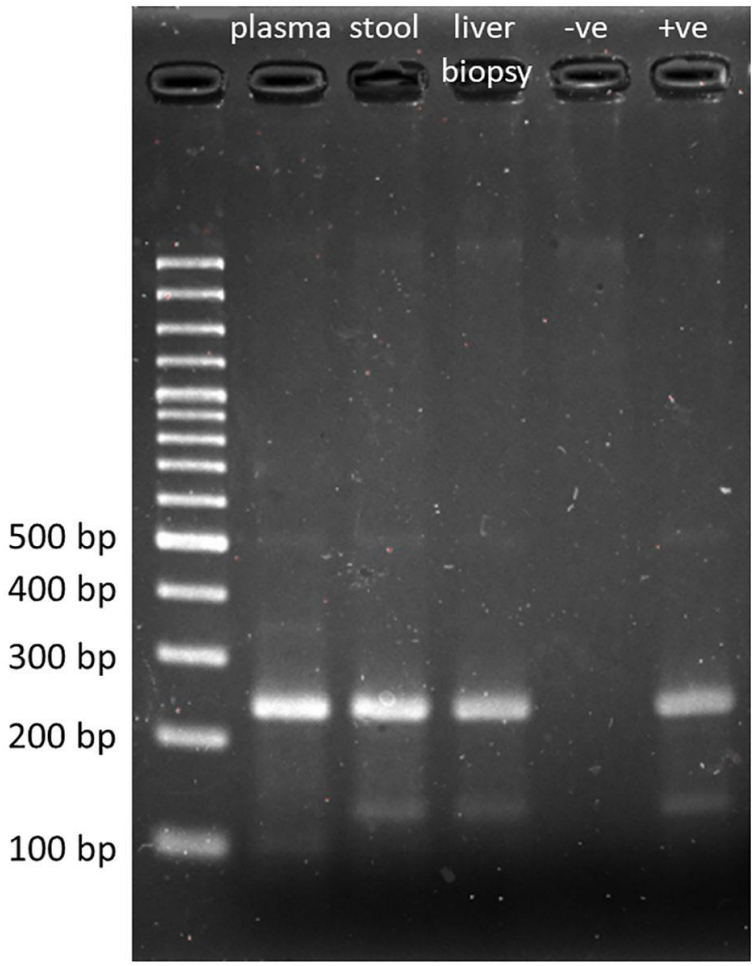

Technical Appendix Figure 1. Detection of hepatitis E virus–C RNA in patient clinical specimens. Gel photograph showing a 235-bp PCR product in patient plasma, stool, and liver tissue after amplification using pan-*Orthohepevirus* primers. –ve: negative control. +ve: positive control

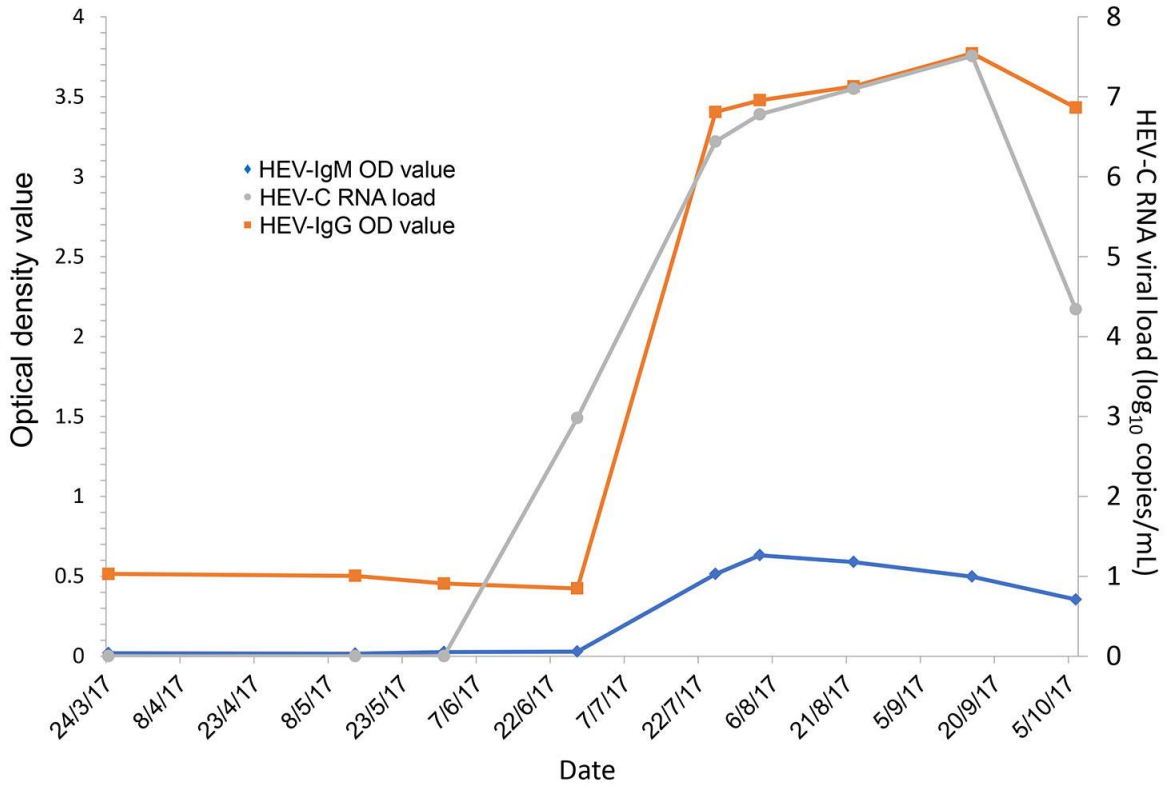

Technical Appendix Figure 2. Wantai HEV IgM and IgG OD values and HEV-C blood RNA loads over time. HEV-C RNA loads in peripheral blood continuously rose despite significant production of HEV IgG as measured by the commercially available Wantai HEV IgG ELISA kit, which uses antigens based on HEV-A. HEV, hepatitis E virus; OD, optical density.

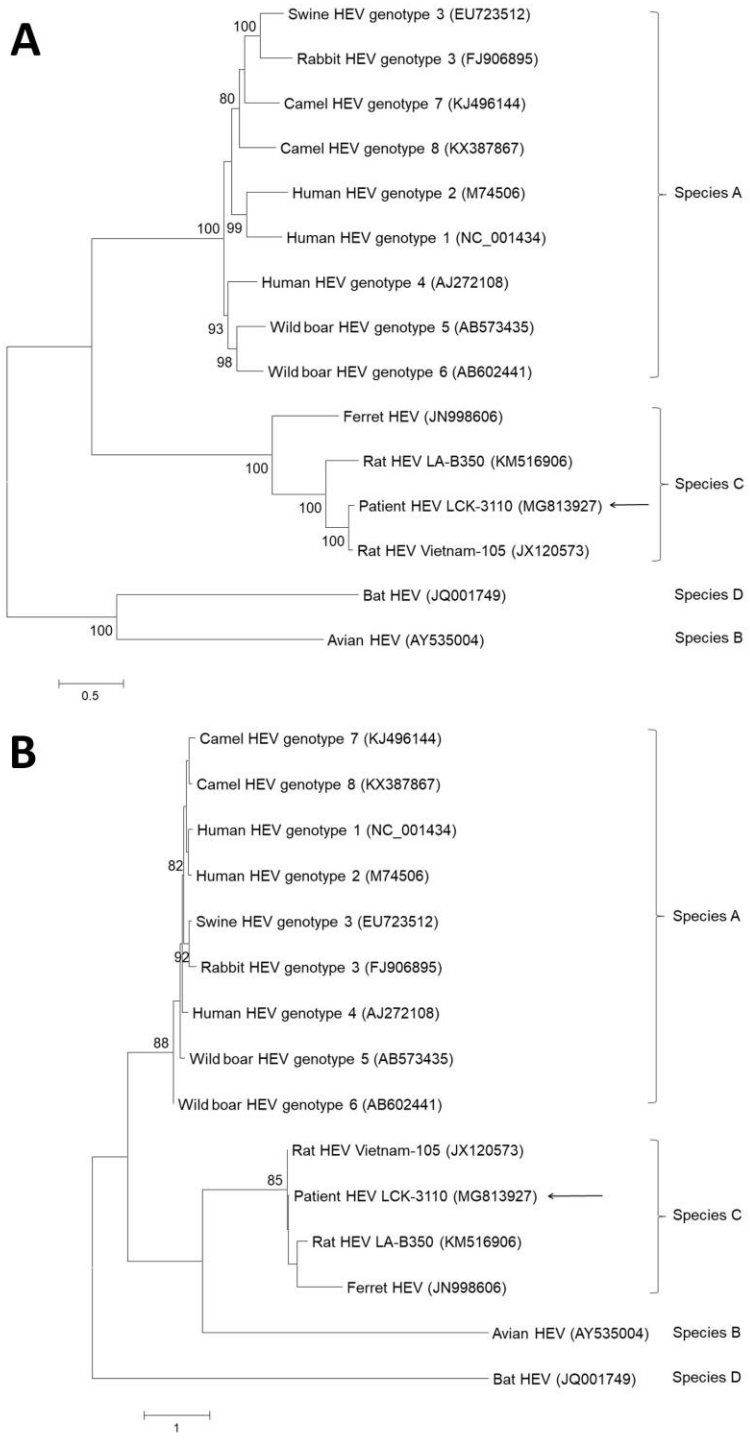

Technical Appendix Figure 3. Phylogenetic analysis using complete (A) open reading frame (ORF) 1 and (B) ORF3 nucleotide sequences of LCK-3110 and other HEV strains. The trees were constructed using maximum-likelihood method with the model GTR+G, with bootstrap values calculated from 1,000 trees. Only bootstrap values >70% are shown. Arrows indicate the strain LCK-3110. HEV, hepatitis E virus. Scale bar indicates nucleotide substitutions per site.

Technical Appendix Figure 4. Multiple sequence alignment of open reading frame (ORF) 2 of HEV genotype 1 (HEV-A), rat HEV (HEV-C) and primer and probe sequences (for HEV-A detection). Primer and probe sequences were adopted from (A) Jothikumar et al., (B) Rolfe et al., (C) Mansuy et al. and (D) Colson et al. HEV, hepatitis E virus.

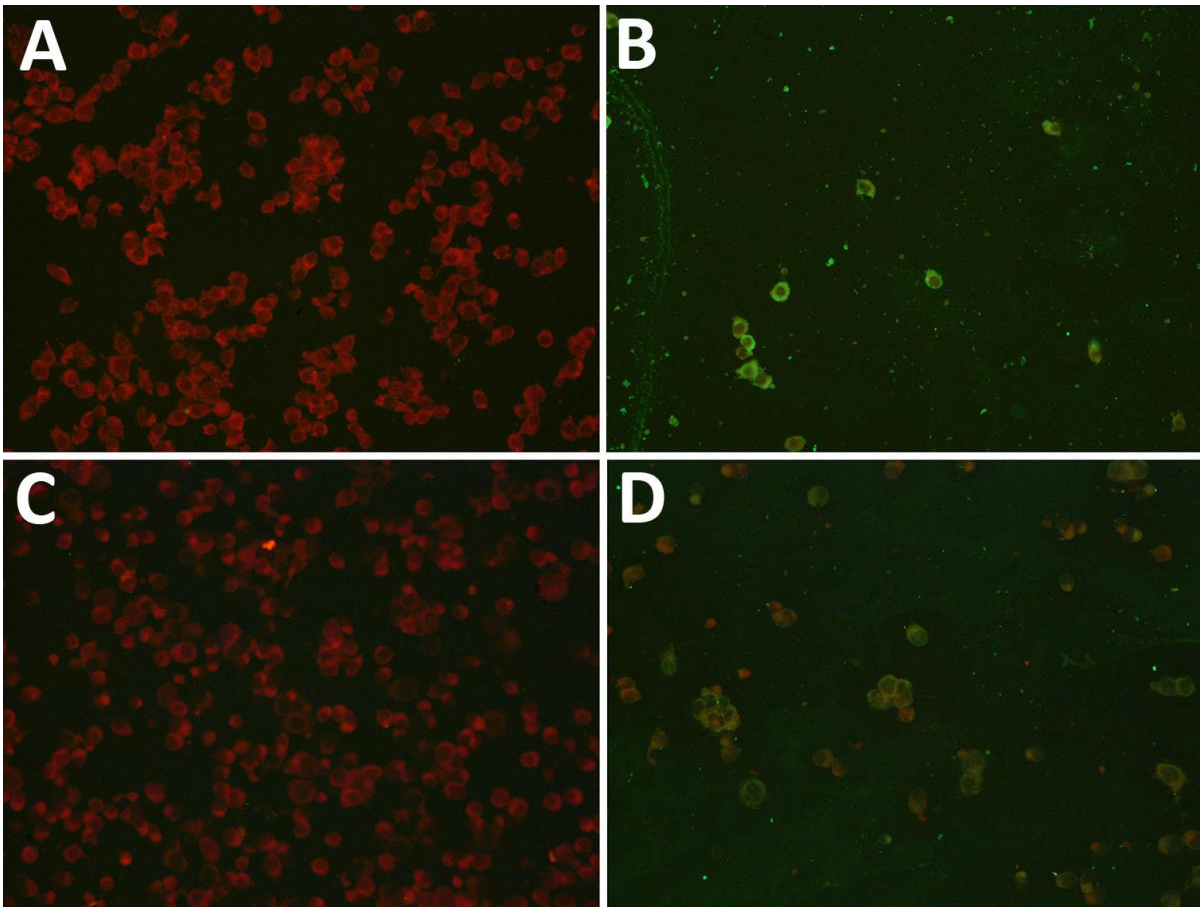

Technical Appendix Figure 5. Immunofluorescence staining of cell culture lysates. Uninoculated permeabilized Huh-7 cells (A) were stained with anti–hepatitis E virus–C (anti–HEV-C) polyclonal antiserum; Huh-7 cells harvested after 7 days of inoculation with patient's stool filtrate were stained with anti-HEV-C polyclonal antiserum (B). Uninoculated permeabilized Caco-2 cells (C) were stained with anti-HEV-C polyclonal antiserum; Caco-2 cells harvested after 7 days of inoculation with patient's stool filtrate were stained with anti-HEV-C polyclonal antiserum.